Front. Energy 2012, 6(4): 420–426
DOI 10.1007/s11708-012-0192-z

RESEARCH ARTICLE

K. YAHIA, S. ZOUZOU, F. BENCHABANE

Induction motors variable speed drives diagnosis through rotor resistance monitoring

Abstract Induction motor driven by vector control method makes high performance control of torque and speed possible. The decoupling of flux and electromagnetic torque obtained by field orientation depends on the precision and the accuracy of the estimated states. Rotor asymmetries lead to perturbations of air gap flux patterns in induction machines. These perturbations in flux components affect the electromagnetic torque, as well as stator currents and voltages. This paper first investigates the control of the induction motor using an extended Kalman filter (EKF) for a direct field-oriented control. It then studies the broken rotor bars (BRBs) fault by the monitoring the rotor resistance. The hypothesis on which the detection is based is that the apparent rotor resistance of the motor will increase when a rotor bar breaks. The rotor resistance is estimated and compared with its nominal value to detect BRBs fault. The EKF estimates the rotor flux, speed and rotor resistance on line by using only measurements of the stator voltages and currents. Simulation results show the effectiveness of the proposed method in the cases of load torque perturbation and speed reversion.

Keywords induction motor, vector control, broken rotor bars (BRBs) diagnostic, extended Kalman filter (EKF)

Received February 28, 2012; accepted April 26, 2012

K. YAHIA (✉), S. ZOUZOU
GEB Laboratory, Department of Electrical Engineering, University of Biskra, BP 145, Biskra, Algeria
E-mail: kd_yahia@yahoo.fr

F. BENCHABANE
MSE Laboratory, Department of Electrical Engineering, University of Biskra, BP 145, Biskra, Algeria

1 Introduction

AC induction motors (IMs) have been widely used in industrial applications such as machine tools, steel mills and paper machines owing to their good performance provided by their solid architecture, low moment of inertia, low ripple of torque and high initiated torque. Some control techniques have been developed to regulate these induction motors drives in high performance applications. One of the most popular techniques is the field-oriented control (direct and indirect) method.

Direct and indirect vector control methods for the speed and torque control of IM have found intensive application through the last three decades. For the indirect control of IM, in addition to the rotor speed, accurate knowledge of the slip frequency (calculated as a function of IM parameters) is required. On the other hand, direct control of IM necessitates accurate information on the rotor speed, as well as rotor flux referring to the stator stationary frame [1,2].

Accurate speed information is necessary to realize high performances and high precision speed control of an induction motor. The speed is achieved by using mechanical sensors such as shaft encoder or resolver. However these sensors are usually expensive, bulky and degrade the system reliability, especially in hostile environment. Thus the sensorless control (involving an estimation of speed) becomes a major subject and an attractive task to industrial applications. Since 1980's, speed sensorless control methods of induction motors using the estimated speed instead of the measured speed have been studied. They have estimated the speed from the instantaneous values of stator voltages and currents using the induction motor model.

Model reference adaptive systems (MRASs) [3] are methods that have a good performance over a large speed range. Their disadvantage is the strong influence of parameter deviation at low speed and standstill operation. Also, the use of PI controllers with complicated gains creates difficulties in their implementation using digital signal processor (DSP) or microcontrollers.

Artificial intelligence methods [4] that use artificial intelligence techniques such as fuzzy logic and neural networks are very promising candidates to be robust to parameter deviation and measurement noise, but they need long development times and an expertise in several artificial intelligence procedures.

Adaptive sliding-mode observer [5] seems to have a very good performance over the full speed range because of the sliding-mode technique; however, the calculation of several gains is needed. Besides, the use of very small gain values results in serious problems during implementation.

The electromagnetic torque of an induction motor can be computed by the knowledge of some variables on the motor such as stator currents and stator flux, stator currents and rotor flux. Stator flux can be evaluated using line to line voltages of the power supply. On other hand, the rotor flux can be evaluated using currents and voltages of the power supply with the knowledge of the mechanical rotation speed [6].

Critical induction motor applications are found in all industries and include all motor horsepowers. It has been found that many of the commercial products to monitor induction motors are not cost-effective when deployed on typical low-to-medium horsepower induction motors. Advances in sensors, algorithms, and architectures should provide the necessary technologies for effective incipient failure detection [7].

This paper, first presents an extended Kalman filter (EKF) for the direct filed-oriented control of an IM. This observer estimates the rotor flux and speed. It, then, uses the observer for the motor rotor resistance estimation in order to perform online BRBs fault monitoring and detection.

2 Induction motor model

The fourth order dynamic model for induction machine developed in stationary reference frame (α, β) is as follows [8,9]:

$$\begin{aligned} \dot{\boldsymbol{x}} &= \boldsymbol{A}\boldsymbol{x} + \boldsymbol{B}\boldsymbol{u}, \\ \boldsymbol{y} &= \boldsymbol{C}\boldsymbol{x}, \end{aligned} \tag{1}$$

where $\boldsymbol{x} = [i_{s\alpha} \quad i_{s\beta} \quad \psi_{r\alpha} \quad \psi_{r\beta}]^{T}$, $\boldsymbol{u} = [u_{s\alpha} \quad u_{s\beta}]^{T}$, $\boldsymbol{y} = [i_{s\alpha} \quad i_{s\beta}]^{T}$, with $\boldsymbol{x}$, $\boldsymbol{u}$, and $\boldsymbol{y}$ being the state vector, the input vector and the output vector, respectively.

$$\boldsymbol{A} = \begin{bmatrix} \gamma & 0 & \dfrac{K_1}{T_r} & pK_1\Omega \\ 0 & \gamma & pK_1\Omega & \dfrac{K_1}{T_r} \\ \dfrac{L_m}{T_r} & 0 & -\dfrac{1}{T_r} & -p\Omega \\ 0 & \dfrac{L_m}{T_r} & p\Omega & -\dfrac{1}{T_r} \end{bmatrix},$$

$$\boldsymbol{B} = \frac{1}{\sigma L_s}\begin{bmatrix} 1 & 0 \\ 0 & 1 \\ 0 & 0 \\ 0 & 0 \end{bmatrix}, \ \boldsymbol{C} = \begin{bmatrix} 1 & 0 \\ 0 & 1 \\ 0 & 0 \\ 0 & 0 \end{bmatrix}^{T}, \ \sigma = 1 - \frac{L_m^2}{L_s L_r},$$

$$\gamma = \frac{R_s}{\sigma L_s} + \frac{R_r L_m^2}{\sigma L_s L_r^2}, \ K_1 = \frac{L_m^2}{\sigma L_s L_r}, \ T_r = \frac{L_r}{R_r}.$$

3 Extended Kalman filter for rotor flux, speed and rotor resistance estimation

The EKF can be used for combined state and parameters estimation by treating selected parameters as extra states and forming an augmented state vector. Since Ω is the parameter to be estimated, Ω is augmented into $\boldsymbol{x}$ which becomes

$$\boldsymbol{x} = [i_{s\alpha} \quad i_{s\beta} \quad \psi_{r\alpha} \quad \psi_{r\beta} \quad \Omega]^{T}.$$

Considering the inherent stochastic characteristic of PWM, treating the fundamental as the deterministic input $\boldsymbol{u}$ and all the higher order harmonics as white Gaussian noise $\boldsymbol{w}$, and considering the measurement noise $\boldsymbol{v}$, the dynamic behaviour of the induction motor can be modelled as follows [10]:

$$\begin{aligned} \boldsymbol{x} &= \boldsymbol{f}(\boldsymbol{x},\boldsymbol{u}) + \boldsymbol{w}, \\ \boldsymbol{y} &= \boldsymbol{h}(\boldsymbol{x}) + \boldsymbol{v}, \end{aligned} \tag{2}$$

where

$$\boldsymbol{f}(\boldsymbol{x},\boldsymbol{u}) = \begin{bmatrix} -\gamma i_{s\alpha} + \dfrac{K_1}{T_r}\psi_{r\alpha} + pK_1\Omega\ \psi_{r\beta} + \dfrac{1}{\sigma L_s}u_{s\alpha} \\ -\gamma i_{s\beta} + \dfrac{K_1}{T_r}\psi_{r\alpha} - pK_1\Omega\ \psi_{r\beta} + \dfrac{1}{\sigma L_s}u_{s\beta} \\ \dfrac{L_m}{T_r}i_{s\alpha} - \dfrac{1}{T_r}\psi_{r\alpha} - p\Omega\psi_{r\beta} \\ \dfrac{L_m}{T_r}i_{s\beta} + p\Omega\psi_{r\alpha} - \dfrac{1}{T_r}\psi_{r\beta} \\ p\Omega \end{bmatrix},$$

$$\boldsymbol{h}(\boldsymbol{x}) = \left[i_{s\alpha} \quad i_{s\beta}\right]^{T},$$

$\boldsymbol{w}$ and $\boldsymbol{v}$ are assumed to be stationary, white, and Gaussian noise, and their expectation values are zero.

The covariance matrices $\boldsymbol{Q}$ and $\boldsymbol{R}$ of these noises are defined as

$$\boldsymbol{Q} = \mathbf{cov}(\boldsymbol{w}) = \boldsymbol{E}(\boldsymbol{w}\boldsymbol{w}'), \ \boldsymbol{R} = \mathbf{cov}(\boldsymbol{v}) = \boldsymbol{E}(\boldsymbol{v}\boldsymbol{v}'),$$

where $\boldsymbol{E}(\cdot)$ denotes the expected values.

To use the extended Kalman filter with nonlinear plant models, such as Eq. (2), the model must be linearized about a nominal state trajectory to produce a linear perturbation model.

The EKF estimator, in the discrete form, can be summarized as follows [6,7,11]:

Step 1: Prediction

▪ Prediction of the state vector

$$\hat{\boldsymbol{x}}(k+1/k)=\boldsymbol{f}(\hat{\boldsymbol{x}}(k/k),\boldsymbol{u}(k)). \quad (3)$$

▪ Prediction covariance computation

$$\boldsymbol{P}(k+1/k)=\boldsymbol{F}(k)\boldsymbol{P}(k)\boldsymbol{F}(k)^{\mathrm{T}}+\boldsymbol{Q}, \quad (4)$$

where

$$\boldsymbol{F}(k)=\left.\frac{\partial\boldsymbol{f}(\boldsymbol{x}(k),\boldsymbol{u}(k))}{\partial\boldsymbol{x}^{\mathrm{T}}(k)}\right|_{\boldsymbol{x}(k)=\hat{\boldsymbol{x}}(k/k)},$$

$$\boldsymbol{F}(k)=\begin{bmatrix}1-T_{\mathrm{s}}\gamma & 0 & T_{\mathrm{s}}\frac{K_1}{T_{\mathrm{r}}} & T_{\mathrm{s}}pK_1\Omega & T_{\mathrm{s}}pK_1\psi_{\mathrm{r}\beta}\\ 0 & 1-T_{\mathrm{s}}\gamma & -T_{\mathrm{s}}pK_1\Omega & T_{\mathrm{s}}\frac{K_1}{T_{\mathrm{r}}} & -T_{\mathrm{s}}pK_1\psi_{\mathrm{r}\alpha}\\ T_{\mathrm{s}}\frac{L_{\mathrm{m}}}{T_{\mathrm{r}}} & 0 & 1-T_{\mathrm{s}}\frac{1}{T_{\mathrm{r}}} & -T_{\mathrm{s}}p\Omega & -T_{\mathrm{s}}p\psi_{\mathrm{r}\beta}\\ 0 & T_{\mathrm{s}}\frac{L_{\mathrm{m}}}{T_{\mathrm{r}}} & T_{\mathrm{s}}p\Omega & 1-T_{\mathrm{s}}\frac{1}{T_{\mathrm{r}}} & T_{\mathrm{s}}p\psi_{\mathrm{r}\alpha}\\ 0 & 0 & 0 & 0 & 1\end{bmatrix}.$$

Step 2: Filtering

The second step (Filtering) corrects the predicted state estimate and its covariance matrix trough a feedback correction scheme that makes use of the actual measured quantities; this is realized by the following recursive relations:

▪ Kalman gain computation

$$\boldsymbol{K}(k+1)=\boldsymbol{P}(k+1/k)\boldsymbol{H}(k)^{\mathrm{T}}\cdot\left(\boldsymbol{H}(k)\boldsymbol{P}(k+1/k)\boldsymbol{H}(k)^{\mathrm{T}}+\boldsymbol{R}\right)^{-1}. \quad (5)$$

▪ State vector estimation (filtering)

$$\hat{\boldsymbol{x}}(k+1/k+1)=\hat{\boldsymbol{x}}(k+1/k)+\boldsymbol{K}(k+1)(\boldsymbol{y}(k+1)-\boldsymbol{H}\hat{\boldsymbol{x}}(k+1/k)). \quad (6)$$

▪ Estimation covariance computation

$$\boldsymbol{P}(k+1/k+1)=\boldsymbol{P}(k+1/k)-\boldsymbol{K}(k+1)\boldsymbol{H}(k)\boldsymbol{P}(k+1/k), \quad (7)$$

where

$$\boldsymbol{H}(k)=\left.\frac{\partial\boldsymbol{h}(x(k))}{\partial\boldsymbol{x}(k)}\right|_{\boldsymbol{x}(k)=\hat{\boldsymbol{x}}(k)},$$

$$\boldsymbol{H}(k)=\begin{bmatrix}1 & 0 & 0 & 0 & 0\\ 0 & 1 & 0 & 0 & 0\end{bmatrix},$$

and k/k denotes a prediction at time k based on data up to time k. Similarly, $(k+1)/k$ denotes a prediction at time $k+1$ based on data up to time k.

The EKF can be used for combined state and parameters estimation by treating selected parameters as extra states and forming an augmented state vector. Since R_{r} is the parameter to be estimated, R_{r} is augmented into $\boldsymbol{x}(k)$ which becomes

$$\boldsymbol{x}(k)=[i_{\mathrm{s}\alpha}(k)\quad i_{\mathrm{sb}}(k)\quad \psi_{\mathrm{r}\alpha}(k)\quad \psi_{\mathrm{rb}}(k)\quad R_{\mathrm{r}}(k)]^{\mathrm{T}}=[x_1(k)\quad x_2(k)\quad x_3(k)\quad x_4(k)\quad x_5(k)]^{\mathrm{T}}. \quad (8)$$

The dynamic behavior of three-phase can be modeled as

$$\begin{aligned}\boldsymbol{x}(k+1)&=\boldsymbol{f}(\boldsymbol{x}(k),\boldsymbol{u}(k))+\boldsymbol{w}(k),\\ \boldsymbol{y}(k)&=\boldsymbol{h}(\boldsymbol{x}(k))+\boldsymbol{v}(k),\end{aligned} \quad (9)$$

where

$$\boldsymbol{f}\left(\boldsymbol{x}(k),\boldsymbol{u}(k)\right)=\begin{bmatrix}\left(1-T_{\mathrm{s}}(\gamma_1+\gamma_2x_5)\right)x_1+T_{\mathrm{s}}\frac{K_1}{L_{\mathrm{r}}}x_5x_3+T_{\mathrm{s}}pK_1\Omega x_4+\frac{T_{\mathrm{s}}}{\sigma L_{\mathrm{s}}}v_{\mathrm{s}\alpha}\\ \left(1-T_{\mathrm{s}}(\gamma_1+\gamma_2x_5)\right)x_2-T_{\mathrm{s}}pK_1\Omega x_3+T_{\mathrm{s}}\frac{K_1}{L_{\mathrm{r}}}x_5x_4+\frac{T_{\mathrm{s}}}{\sigma L_{\mathrm{s}}}v_{\mathrm{s}\beta}\\ T_{\mathrm{s}}\frac{L_{\mathrm{m}}}{L_{\mathrm{r}}}x_5x_1+\left(1-\frac{T_{\mathrm{s}}}{L_{\mathrm{r}}}x_5x_3\right)-T_{\mathrm{s}}p\Omega x_4\\ T_{\mathrm{s}}\frac{L_{\mathrm{m}}}{L_{\mathrm{r}}}x_5x_2+T_{\mathrm{s}}p\Omega x_3\left(1-T_{\mathrm{s}}\frac{1}{L_{\mathrm{r}}}x_5x_4\right)\\ x_5\end{bmatrix}, \quad (10)$$

$$\boldsymbol{F}(k)=\begin{bmatrix} 1-T_s(\gamma_1+\gamma_2x_5) & 0 & T_s\frac{K_1}{L_r}x_5 & T_spK_1\Omega & T_s\left(\frac{K_1}{L_r}x_3-\gamma_2x_1\right) \\ 0 & 1-T_s(\gamma_1+\gamma_2x_5) & -T_spK_1\Omega & T_s\frac{K_1}{L_r}x_5 & T_s\left(\frac{K_1}{L_r}x_4-\gamma_2x_2\right) \\ T_s\frac{L_m}{L_r}x_5 & 0 & 1-\frac{T_s}{L_r}x_5 & T_sp\Omega & T_s\left(\frac{L_m}{L_r}x_1-\frac{T_s}{L_r}x_3\right) \\ 0 & T_s\frac{L_m}{L_r}x_5 & T_sp\Omega & 1-\frac{T_s}{L_r}x_5 & T_s\left(\frac{L_m}{L_r}x_2-\frac{T_s}{L_r}x_4\right) \\ 0 & 0 & 0 & 0 & 1 \end{bmatrix}, \tag{11}$$

where

$$\boldsymbol{H}(k)=\left.\frac{\partial \boldsymbol{h}(\boldsymbol{x}(k))}{\partial \boldsymbol{x}(k)}\right|_{\boldsymbol{x}(k)=\tilde{\boldsymbol{x}}(k)}=\begin{bmatrix} 1 & 0 & 0 & 0 & 0 \\ 0 & 1 & 0 & 0 & 0 \end{bmatrix}. \tag{12}$$

4 Simulation results

The EKF is applied to an induction motor direct field oriented controlled as shown in Fig. 1. This observer first estimates the rotor flux and speed of a reliable variable speed drive, and then the induction motor rotor resistance for BRBs fault diagnosis.

The dynamic behavior of the sensorless controller with speed reversal from 100 to -100 rad/s at 0.4 s for unloaded induction motor is illustrated in Fig. 2, which shows the real and estimated speed, the speed estimation error, the real and estimated flux in (α,β) reference frame, the real and estimated flux modulo and its estimation error, the torque and fluxes in (d,q) reference frame. It can be noticed that the acceptable speed estimation error is in a steady state. In starting and reversing times, this error is also negligible. The flux estimation is done with a good accuracy. Therefore, this observer demonstrates and guarantees good performances of regulation and a high stability of the global system.

EKF implementation needs the best choice of the covariance matrices $\boldsymbol{Q}$ and $\boldsymbol{R}$. The noise covariance $\boldsymbol{R}$ accounts for the measurement noise introduced by the current sensors and quantization errors of the A/D converters [2]. The increase in $\boldsymbol{R}$ indicates stronger disturbance of the current. The noise is weighted less by the filter, causing also a slower transient performance of the system. The noise covariance $\boldsymbol{Q}$ reflects the system model inaccuracy, the errors of the parameters and the noise introduced by the voltage estimation [6]. $\boldsymbol{Q}$ has to be increased at a stronger noise in driving the system, entailing a more heavily weighting of the measured current and a faster transient performance. An initial matrix $\boldsymbol{P}_0$

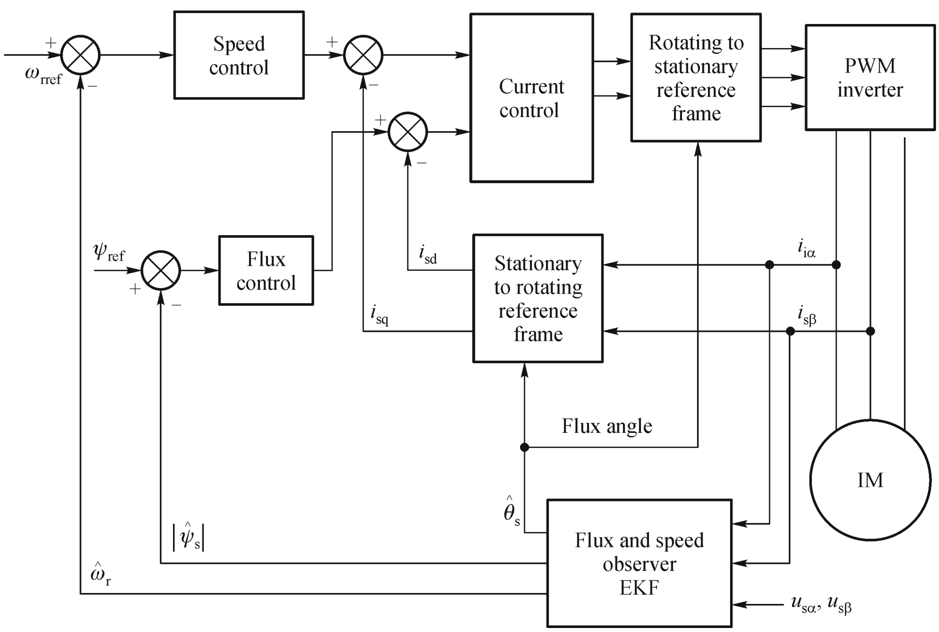

Fig. 1 Speed control of an induction machine using direct field-oriented control method based on an EKF

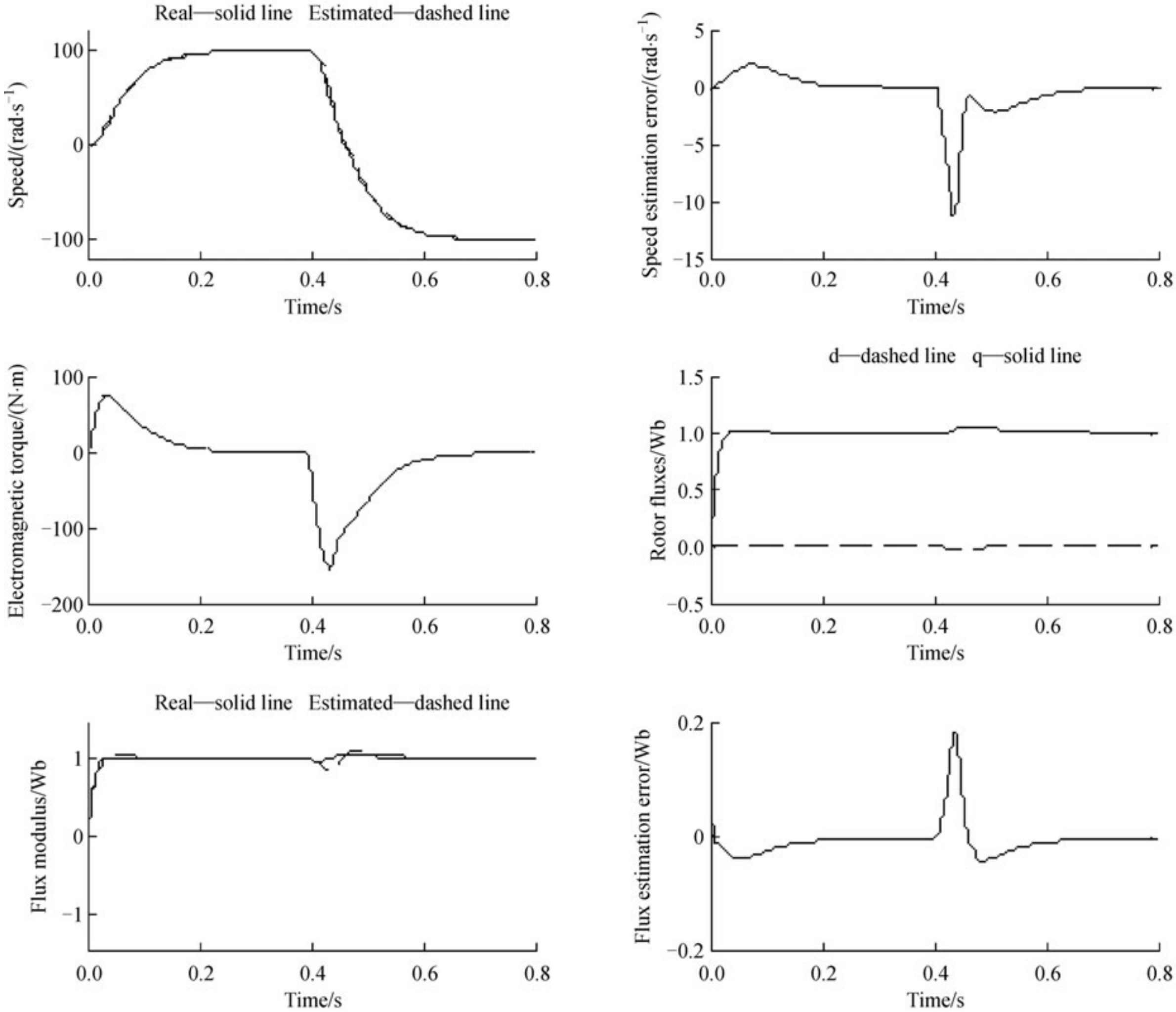

Fig. 2 Dynamic behavior of the sensorless controller with speed reversal from 100 to −100 rad/s at 0.4 s for unloaded induction motor

represents the matrix of the covariance in knowledge of the initial condition. Varying $\boldsymbol{P}_0$ affects neither the transient performance nor the steady state condition of the system. In this study, the value of these elements is tuned "manually", by running several simulations. This is probably one of the major drawbacks of the Kalman filter.

The sensorless controller characteristics for speed step response of 100 rad/s with 0.4 and 0.8 s applied load of 10 and 25 N·m respectively are depicted in Fig. 3, which shows the estimation error of speed and flux modulo, the real and estimated torque and the flux angle. From Fig. 3, a good estimation of the motor speed can be noticed with a few rad/s errors in transient state and when load is applied but globally the robustness and accuracy are well achieved.

The tracking of the rotor resistance variations, when the rotor resistance value of the IM is changed linearly when $R_r(t) = R_{rn}t + 1.3\ (\Omega)$ is demonstrated in Fig. 4. The Kalman filter capability to track linear profile has been tested. This fact presents a slowly failure (damage) of the rotor bar. It can be noticed that the estimation accuracy is quite satisfactory for monitoring purposes.

Figure 5 displays the tracking of the rotor resistance variations, when the rotor resistance value of IM is changed abruptly: stepped-up by 50% of its initial value in 1 s and by 100% of its initial value in 2 s. This result suggests that even if the rotor resistance changes abruptly, the EKF still gives a good estimation of this parameter. As it is well known, the BRBs can increase abruptly the rotor resistance. Therefore, the EKF can be used to diagnose the motor by monitoring the change in the rotor resistance.

5 Conclusions

The detailed design procedure for the extended Kalman filter has been presented and used for the speed sensorless direct vector control of an induction motor. It can be concluded from the simulation results that the estimation of

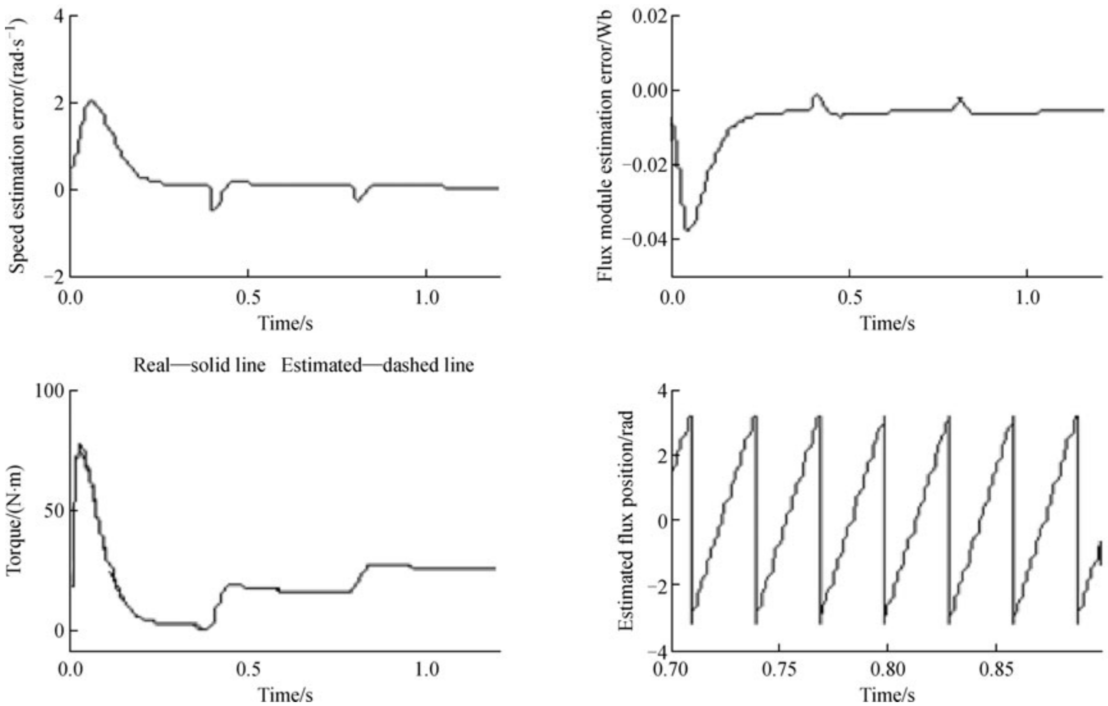

Fig. 3 Dynamic behaviour of the sensorless controller with maximum speed reference equalling 100 rad/s and applied load torque equalling 10 N·m at 0.4 s and 25 N·m at 0.8 s

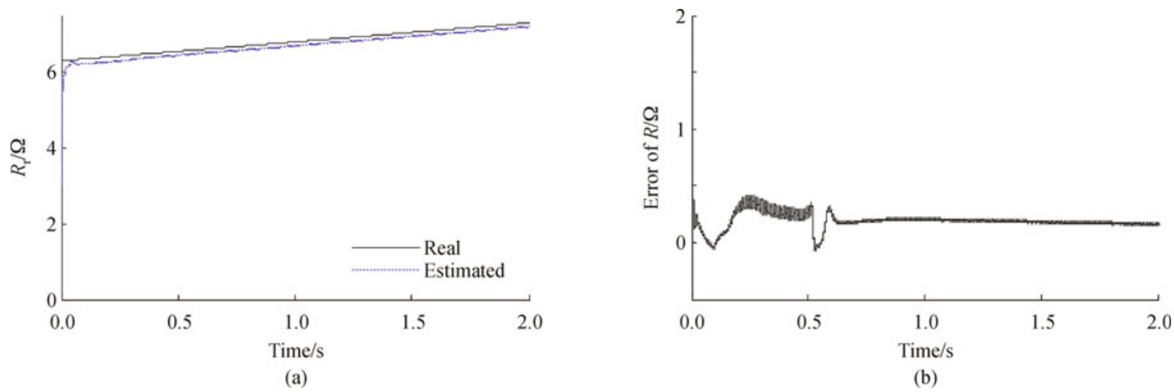

Fig. 4 Induction motor rotor resistance estimation with a rotor resistance linear profile variation for a full loaded motor (a) Real and estimated resistances; (b) estimation error

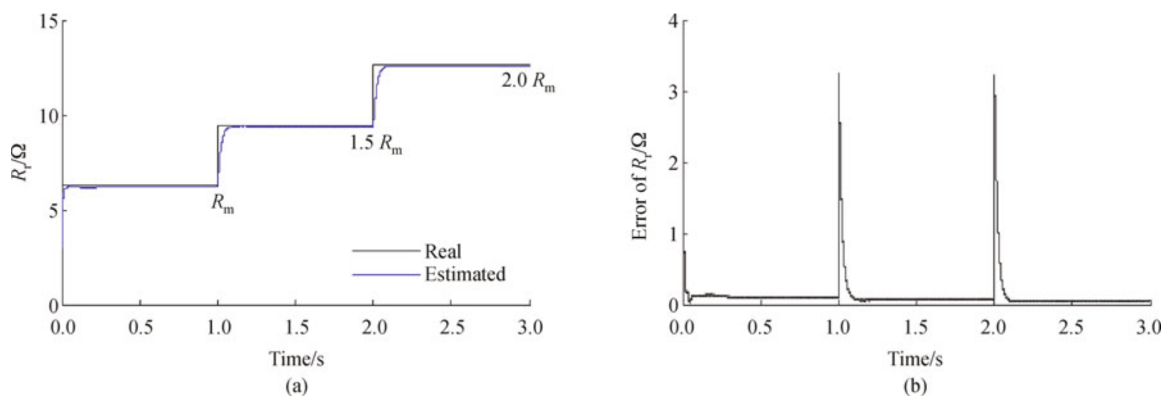

Fig. 5 Induction motor rotor resistance estimation with a rotor resistance step profile variation for a full loaded motor (a) Real and estimated resistances; (b) estimation error

rotor flux and rotor speed has been done satisfactory. The global system drive is stable and robust against load perturbation and speed reversion. The EKF has been also used to estimate the rotor resistance in order to perform an online diagnosis of the induction motor. Given that the increase in the rotor resistance gives information regarding the condition of motor rotor, rotor resistance is estimated and compared with its nominal value to detect broken bars. Simulation results have shown good performances of rotor resistance estimation for both linear and step variation profiles. The proposed EKF method provides a reliable BRBs fault diagnosis.

Appendix

The induction motor used for the simulation studies has the following parameters:

Type: Three-phase, 4 kW. 220/380 V, squirrel-cage induction motor.

$$R_s = 1.2\ \Omega;\ R_r = 6.3\ \Omega;\ L_s = 0.1554\ \text{H};$$

$$p = 2;\ L_r = 0.1568\ \text{H};\ L_m = 0.15\ \text{H};$$

$$J = 0.07\ \text{kg}\cdot\text{m}^2;\ f_r = 0.001\ \text{N}\cdot\text{m}\cdot\text{s/rad};$$

$$T_l = 25\ \text{N}\cdot\text{m};\ \Omega = 150\ \text{rad/s}.$$

The following values have been chosen for $\boldsymbol{Q}$ and $\boldsymbol{R}$ matrices:

Covariance matrices

$$\boldsymbol{Q} = [1\text{e}^{-5}\quad 1\text{e}^{-5}\quad 1\text{e}^{-5}\quad 1\text{e}^{-5}\quad 1\text{e}^{-1}],$$

$$\boldsymbol{R} = [1\quad 1],\ T_s = 1\text{e}^{-4}\ \text{s}.$$

Notations

$i_{s\alpha\beta} = i_{s\alpha} + \text{j}i_{s\beta}$	(α,β) stator current vector
$u_{s\alpha\beta} = u_{s\alpha} + \text{j}u_{s\beta}$	(α,β) stator voltage vector
$\boldsymbol{w},\boldsymbol{v}$	State and output noise vectors
$\boldsymbol{y}(k)$	Output matrix of the linearised augmented model
C_e	Electromagnetic torque
$\boldsymbol{F}(k)$	System matrix of the linearised augmented model
$\boldsymbol{G}$	Observer gain matrix
J	Shaft inertia
$\boldsymbol{K}(k)$	Optimal Kalman gain matrix
L_m	Magnetising inductance
L_r	Rotor self inductance
L_s	Stator self inductance
P	Number of pole pairs
$\boldsymbol{P}(k)$	State estimation error covariance matrix
$\boldsymbol{Q}$, $\boldsymbol{R}$	State noise and output noise covariance matrices
R_r	Rotor phase resistance
R_s	Stator phase resistance
T_l	Load torque
T_s	Sampling time
σ	Total leakage factor
$\psi_{r\alpha\beta} = \psi_{r\alpha} + \text{j}\psi_{r\beta}$	(α,β) rotor flux vector
ω_r	Electrical rotor speed
Ω	Mechanical rotor speed

References

1. Zai L C, Demarco C L, Lipo T A. An extended Kalman filter approach to rotor time constant measurement in PWM induction motor drives. IEEE Transactions on Industry Applications, 1992, 28 (1): 96–104
2. Akin B. State estimation techniques for speed sensorless field oriented control of induction motors. Dissertation for the Master's Degree. Ankara, Turkey: The Middle East Technical University, 2003
3. Schauder C. Adaptive speed identification for vector control without rotational transducers. IEEE Transactions on Industry Applications, 1992, 28(05): 1176–1185
4. Vas P. Artificial-Intelligence-Based Electrical Machines and Drives-Application of Fuzzy, Neural, Fuzzy-Neural and Genetic-Algorithm-Based Techniques. Oxford: Oxford University Press, 1999
5. Xepaps A, Kaletsanos A, Xepaps F, Manias S. Sliding–mode observer for speed sensorless induction motor drives. IEE Proceedings. Control Theory and Applications, 2003, 150(6): 611–661
6. Yahia K. On line estimation of state and parameters of a three phase asynchronous motor. Dissertation for the Magister's Degree. Biskra, Algeria: Biskra University, 2005
7. Naït Saïd M S, Benbouzid M H, Benchaib A. Detection of broken bars in induction motors using an extended Kalman filter for rotor resistance sensorless estimation. IEEE Transactions on Energy Conversion, 2000, 15(1): 66–70
8. Benchabane F, Titaouine A, Bennis O, Yahia K, Taibi D. Direct field oriented control scheme for space vector modulated AC/DC/AC converter fed induction motor. Frontiers in Energy, 2012, 6(2): 129–137
9. Ohnishi O, Ueda A, Miyachi K. Model reference adaptive system against rotor resistance variation in induction motor drive. IEEE Transactions on Industrial Electronics, 1986, 33(3): 217–223
10. Atkinson D, Acarnley P, Finch J. Observers for induction motor drives. IEEE Transactions on Industrial Electronics, 1991, 27(03): 1119–1127
11. Salvatore L, Stasi S, Tarchiono L. A new EKF-based algorithm for flux estimation in induction machines. IEEE Transactions on Industrial Electronics, 1993, 40(6): 496–504